



Enhanced removal efficiency of bromate from aqueous solutions by nanoscale zero-valent iron immobilized on activated carbon

Chunhua Xu*, Xiaohong Wang, Sheng Lin, Liujiu Zhu, Yaming Chen

Shandong Key Laboratory of Water Pollution Control and Resource Reuse, School of Environmental Science and Engineering, Shandong University, Jinan 250100, China, Tel. +86 531 88362170; Fax: +86 531 88364513; email: xuchunhua@sdu.edu.cn

Received 5 May 2013; Accepted 1 March 2014

ABSTRACT

Nanoscale zero-valent iron (nZVI) immobilized on activated carbon (AC) was synthesized via liquid phase reduction route. The samples were characterized by X-ray diffraction, transmission electron microscopy, and Brunauer–Emmett–Teller surface area measurement. The effects of bromate (BrO_3^-) removal in water with nZVI/AC samples were evaluated. The results show that nZVI/AC presented superior bromate removal efficiency, which is contributed to its reduction and synergistic adsorption/sedimentation of BrO_3^- . Iron species in nZVI/AC acted as electron mediator and catalyst during bromate reduction, and bromide was the final reductive product. The dosage of nZVI/AC, solution pH, initial bromate concentration, reaction time, and temperature affected the rates of bromate reduction/adsorption. The optimum pH range of bromate removal is wide enough from 4.0 to 9.0. Bromate removal capacity of nZVI/AC was determined to be approximately 25 mg/g. These findings suggest that bromate removal by nZVI/AC can be an effective method for bromate control.

Keywords: Nanoscale zero-valent iron; Activated carbon; Bromate reduction; Adsorption

1. Introduction

Bromate (BrO_3^-) has attracted considerable attention since it is known to induce cancer. It has been classified as a possible carcinogenic substance to humans by both the United States Environmental Protection Agency and the World Health Organization (WHO) [1,2]. BrO_3^- can enter the human body by oral route and the enforceable maximum contaminant level is 10 $\mu\text{g}/\text{L}$ [3]. According to the estimation of WHO, 3 $\mu\text{g}/\text{L}$ BrO_3^- in drinking water corresponds to a cancer risk of 10^{-5} (life-time exposure) [4]. There is no bromate in natural waters, but ozonation can convert bromide to bromate when dealing with water

containing bromide. The formation mechanisms of bromate are very complex which involve in molecular ozone (O_3) and hydroxyl radical ($\text{OH}\bullet$) reactions [5]. Different methods are applied in drinking water purification for bromate removal, such as adsorption by activated carbon (AC) [6] and granular ferric hydroxide [7], reduction using nanoscale zero-valent iron (nZVI) [8–10], ionic exchange [11,12], and UV irradiation [13,14].

In the above-mentioned methods, reduction seems to be the most widely used method for bromate removal. Synthesis and applications of reactive metal particles in remediation of the groundwater and drinking water contaminated by brominated compounds have shown significant environmental implications. ZVI/nZVI has recently been considered

*Corresponding author.

as an effective material for bromate uptake. ZVI is an effective reductant due to its low-redox potential ($E^0 = -0.44$ V). In some circumstances ($E^0 < -0.44$ V), its primary corrosion product (Fe^{2+}) may be a more favorable reductive agent than ZVI because the electrode potentials of the $\text{Fe}_{(s)}^{3+}/\text{Fe}_{(s)}^{2+}$ ($E^0 = \text{Fe}_{(s)}^{3+}/\text{Fe}_{(s)}^{2+}$) is between -0.35 and -0.65 V, and is lower than that of ZVI [15]. In recent years, there has been an increased interest in applying nZVI in removing aqueous contaminants under anoxic condition. nZVI is effective for the removal of organics (e.g. pentachlorophenol, nitrobenzene, 4-chlorobiphenyl, chlorinated ethane, trichloroethylene, perchloroethylene, and 2,4-dinitrotoluene [16–21]) as well as inorganics (e.g. bromate, arsenate, hexavalent chromium, nitrate, carbon disulfide, and selenate [8,10,22–28]) from groundwater and wastewater. Xie and Shang [10] investigated bromate reduction under different conditions and the mechanism of bromate removal by ZVI with the pseudo-first-order kinetics model. But Wang et al. [18] obtained the bromate reduction using nZVI by fitting it in a second-order kinetic model.

Besides the strong reduction ability, nZVI is also considered as a promising adsorption material due to its high-specific surface area [29]. However, the occurrence of nZVI in fine particles and the aggregation of nZVI inhibited its practical application. Hence, loading nZVI onto supporting materials could be an effective method for convenient applications [29–31]. The supporting material may prevent agglomeration of nZVI and provides higher specific surface area and activity [32], while the bound nZVI performs the reduction. Zhu et al. [29] and Gu et al. [33] reported the supported nZVI on AC for arsenic removal from drinking water. The results showed that the composite material was effective for arsenic removal with relatively fast kinetics reaction rate [29]. Hoch et al. [30] synthesized carbon-supported nZVI particles for the remediation of Cr(VI), and the results demonstrated that the reactive nano iron can be made in a scalable process from inexpensive starting materials. Shi et al. [31] used bentonite as the support material to synthesize B-nZVI composite, and kinetics studies showed that reduction of Cr(VI) to Cr(III) could be expressed by pseudo-first-order reaction kinetics.

However, there were few reports about the application of nZVI/AC in bromate removal and the influence of different loads of nZVI on AC to the bromate removal. In this study, nZVI/AC was prepared by borohydride reduction of an aqueous iron salt when AC was in the reaction system. And it was used for bromate reduction; the different loads of nZVI on AC were also introduced to explore the best load for bromate removal. The impact factors during bromate

removal were also studied to obtain the optimum condition.

2. Experimental section

2.1. Materials and chemicals

Ferrous sulfate ($\text{FeSO}_4 \cdot 7\text{H}_2\text{O}$, 99.5%, GR, Tianjin Kermel Chemical Reagent Co., China), PEG-4000 (CP, Shantou Xilong Chemical Factory, China), potassium borohydride (KBH_4 , 95%, CP, Sinopharm Chemical Regent Co. Ltd, China), absolute ethanol ($\text{CH}_3\text{CH}_2\text{OH}$, 99.7%, CP, Tianjin Damao Chemical Regent Factory, China), sodium hydroxide (NaOH , AR, Jinan Regent Central Factory, China), hydrochloric acid (HCl , AR, Tianjin Fuyu Chemical Co. Ltd, China), bromate (NaBrO_3 , AR, Tianjin Kermel Chemical Reagent Co. Ltd, China), the respective chemicals were obtained from respective companies. The commercial powder activated carbon (AC, AR) was obtained from Tianjin Dengke Chemical Regent Co. Ltd, (China), which is used as the supporting material for coating nZVI. General nitrogen (N_2 , purity 99.5%, Jinan Deyang Special Gas Co. Ltd, China) was used as protective gas. The AC should be pretreated with HCl before using.

2.2. Preparation of nZVI and nZVI/AC

The nZVI was prepared by reduction of an aqueous ferrous iron solution using NaBH_4 based on a slightly modified method [34,35]. In a typical synthesis route: in a 500 mL four-necked open flask, 1.1912 g $\text{FeSO}_4 \cdot 7\text{H}_2\text{O}$ was dissolved in 60 mL ethanol/deionized water mixture (V/V 4/1). 0.2 g PEG-4000 was then added into the above solution as dispersant. The solution pH was adjusted to 6.5 with 1 M NaOH aqueous solution. Subsequently, 33 mL of 0.9255 g KBH_4 aqueous solution was added dropwise (1 drop/s) while stirring vigorously (220 rpm). Then, the solution was stirred for another 30 min at room temperature. The resulting black solid was collected by magnetic separation and washed with deoxygenated water three times and deoxygenated absolute ethanol twice, respectively. Finally, the nZVI slurry was dried at 70°C and stored in a N_2 -purged chamber before use. The whole process described above was conducted under a N_2 atmosphere to prevent nZVI oxidation from atmospheric oxygen.

To prepare nZVI/AC, the AC was first put into 5 M HCl and was heated and boiled on the furnace for 20 min, then washed with deionized water and dried overnight at 120°C . After that, 0.9598 g AC was immersed in 60 mL ethanol/deionized water mixture (V/V 4:1) which has dissolved 1.1912 g $\text{FeSO}_4 \cdot 7\text{H}_2\text{O}$,

and then the suspension liquid was stirred for at least 30 min. The following steps are the same with those described above. The theoretical mass fraction of Fe^0 in the obtained nZVI/AC composites prepared is above 25% (by weight). To synthesize 20 and 30% loading of nZVI onto AC, we can simply adjust the amount of AC to 1.1912 and 0.7998 g, respectively, without changing other conditions. The nZVI/AC with different iron loadings of 20, 25, and 30% (mass fraction) were marked nZVI/AC-1, nZVI/AC-2, and nZVI/AC-3, respectively.

2.3. Physical characterization

X-ray diffraction (XRD) analyses were conducted in an ambient air with $\text{Cu-K}\alpha$ using a Rigaku RINT2000 wide-angle goniometer with continuous scans from 10° to 70° . The scanning rate was set at $8.0^\circ/\text{min}$. Transmission electron microscope (TEM) images were obtained using a TEM (JEM-100CX II, Japan). Large-scale morphology was also analyzed by a scanning electron microscope (SEM) (JSM-6510 LV, Japan). The specific surface area of the synthesized adsorbent was measured by the BET methodology using a specific surface area and pore size analyzer (ST-08B, Beijing YFRP Technology Co. Ltd, China).

2.4. Batch experiments for bromate removal

Bromate stock solutions were prepared from reagent grade chemicals using deionized water and stored at 4°C , and a concentration bromate solution (10 mg/L) was obtained by diluting the stock solution before use. All batch experiments were carried out with 100 mL of bromate solution and nZVI/AC of known initial concentrations in 250-mL capped conical flasks with agitation in an ordinary thermostatic rotary shaker (SHZ-82, Jintan Medical Instrument Factory, Jiangsu, China) and a digital freeze water bath thermostatic rotary shaker (SHA-2(A), Jintan Jinnan Instrument Manufacturing Co. Ltd, China) for conducting some experiments at low temperatures. Samples were collected at regular intervals and detected by certain instruments to know bromate, bromide, and total iron levels after filtration using $0.22\ \mu\text{m}$ disposable membrane filters. The concentration of bromate and bromide was analyzed by single-column ion chromatography (IC1010, Shanghai Tianmei Science Instrument Co. Ltd, China), and the total iron levels were measured using an atomic absorption spectrophotometer (TAS-990, Beijing Purkinje General Instrument Co. Ltd, China).

To investigate the effect of the content of nZVI in the composite material on bromate removal, the three aforementioned types of synthesized nZVI/AC were added to a prepared bromate solution (the initial bromate concentration is 10 mg/L) at 298 K. The capped conical flasks were shook at 200 rpm immediately after adding nZVI/AC into 100 mL bromate solutions. Samples were collected at regular intervals, and subjected to instruments to detect the concentrations of BrO_3^- , Br^- , and total iron.

And batch experiments about the effect of different parameters (such as pH, reaction time, initial bromate concentration and temperature) were also conducted to investigate the bromate efficiency by nZVI. The influence of the solution was investigated by adjusting solution pH from 3.0 to 10.0 using 0.1 M HCl or 0.1 M NaOH under an initial bromate concentration of 10 mg/L, adsorbent dosage of 0.4 g/L, and reaction time 20 min at 298 K. The pH was measured before and after the experiments. The effect of nZVI/AC dosage on bromate removal was studied by varying the amount of nZVI/AC from 0.2 to 0.5 g/L, while keeping other parameters such as pH (7.0), initial bromate concentration (10 mg/L), temperature (298 K), and contact time (20 min) constant. After reaction, the concentrations of bromate and bromide were also measured. The effect of initial concentration and different temperature was conducted with changing initial bromate concentrations (1, 5, and 10 mg/L) or temperatures (288, 298, and 308 K) with contact time ranging from 3 to 20 min, and analysis for bromate and bromide samples were taken at regular intervals. All the experiments were conducted in duplicate and the data in the figures were average of the two sets of data.

3. Results and discussion

3.1. Characterization of nZVI and nZVI/AC

3.1.1. XRD and TEM

The synthesized nZVI and nZVI/AC materials were characterized using XRD and TEM. TEM was used to investigate the morphology of pristine nZVI and nZVI/AC, while XRD was used to investigate the material structure of nano iron particles.

Fig. 1 presents XRD of nZVI and nZVI/AC (20% loading). nZVI was characterized by an obvious peak of $\alpha\text{-Fe}^0$ (110) at 44.722 (2-theta degree) as shown in Fig. 1(a). There were no other miscellaneous peaks, which indicated that the nZVI material was not oxidized or that the level of oxidation was extremely low. And the peak of $\alpha\text{-Fe}^0$ (110) illustrates the fineness and good crystallization of materials prepared in

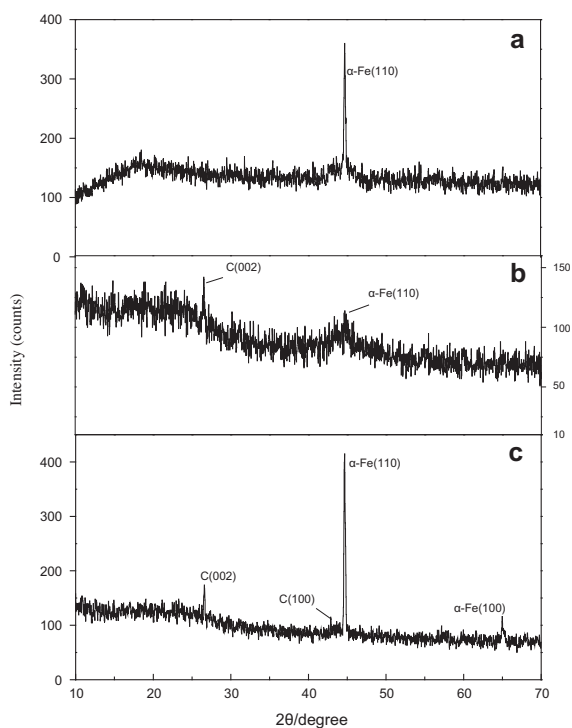


Fig. 1. XRD patterns of nZVI and nZVI/AC: (a) nZVI; (b) nZVI/AC; (c) nZVI/AC, crystallized at high temperature (420 °C).

this method. Compared with the sharp peak of $\alpha\text{-Fe}^0$ nZVI material, the peak of nZVI coated on AC was relatively low as shown in Fig. 1(b). Seen from the Fig. 1(b), the peaks displayed some kind of broadening effect, which indicates morphological characteristics of microcrystal on the composite material. Fig. 1(c) shows the XRD image of nZVI/AC that was crystallized at 420 °C, and $2\theta = 26.562$, $2\theta = 42.942$, $2\theta = 44.661$, and $2\theta = 64.982$ were corresponding C(002), C(100), $\alpha\text{-Fe}(110)$, and $\alpha\text{-Fe}(200)$ crystal surface in turn. Peaks of C(002) and $\alpha\text{-Fe}(110)$ of crystallized nZVI/AC material sharpened in comparison with peaks of nZVI/AC without being crystallized at high temperature. The changes demonstrated above indicated that the temperature can promote the crystallization level of graphite and $\alpha\text{-Fe}$ after drying. As a result, the temperature of crystallization is also an important parameter to control the size of nano iron particles.

Fig. 2 shows the TEM images of pristine nZVI/AC samples. The observed iron particles increased significantly when increasing the loading amount. nZVI formed a chain-like aggregated structure because of its natural tendency to remain in a more thermodynamically stable state [36] in Fig. 2(c).

3.1.2. BET surface area

The BET surface areas of different types of nZVI/AC were analyzed in this study for comparisons (Table 1). As Table 1 shows, the surface area of nZVI increased after coating onto AC due to the augmentation of AC. And nZVI/AC-2 has the biggest surface area among the three types. Hence, nZVI/AC-2 maybe has a better removal efficiency of bromate than the other types.

3.2. Removal of bromate

3.2.1. Effect of Fe on the synthesis of nZVI/AC

The effect of nZVI loading on AC for the removal of bromate was studied using 10 mg/L bromate solution and the mass ratio of nZVI over AC from 20 to 30%, which was marked as nZVI/AC-1, nZVI/AC-2, and nZVI/AC-3. The effects of different nZVI/AC ratio on bromate removal and the total iron concentration were presented in Fig. 3, and the bromide concentrations reduced by different nZVI were presented in Fig. 4. Fig. 3(a) showed that when the ratio of nZVI/AC increased from 20 to 30%, the bromate removal rate was enhanced accordingly; the sharp decreases of BrO_3^- concentrations in the first 15 min were probably due to the increased amount of nZVI on AC reduced bromate into bromide. And the bromate removal efficiency remained stable after 20 min. This implies the bromate could be effectively removed using nZVI/AC within 20 min. The removal efficiency of bromate was increased as we increased the loading of nZVI on AC. This may be attributed to the abundant active sites on the nZVI/AC. Similar articles verified this phenomenon using other nZVI composites [35–38].

Fig. 3(a) also indicates that the bromate removal rates varied with the different nZVI loading on AC. Within 20 min, bromate could be effectively reduced from 10.0 mg/L to about 0.49, 0.23, and 0.02 mg/L by nZVI/AC-1, nZVI/AC-2, and nZVI/AC-3, respectively. Hence, nZVI/AC-2 and nZVI/AC-3 had higher removal efficiency. Because of the reduction of nZVI to bromate, Fe^0 will be oxidized to Fe^{2+} , Fe^{3+} , and all the forms of iron in the solution will appear as total iron in Fig. 3(b). The dissolved iron after reaction was low Fig. 3(b), indicating that most of the iron atoms were combined with AC to form Fe(III) precipitate. Furthermore, as the load of iron increases from 25 to 30%, the aggregation of iron particles on the surface of AC occurs Fig. 2(c). This is adverse to iron participating in the reactions, and the total iron concentration in the solution with nZVI/AC-3 was higher than those

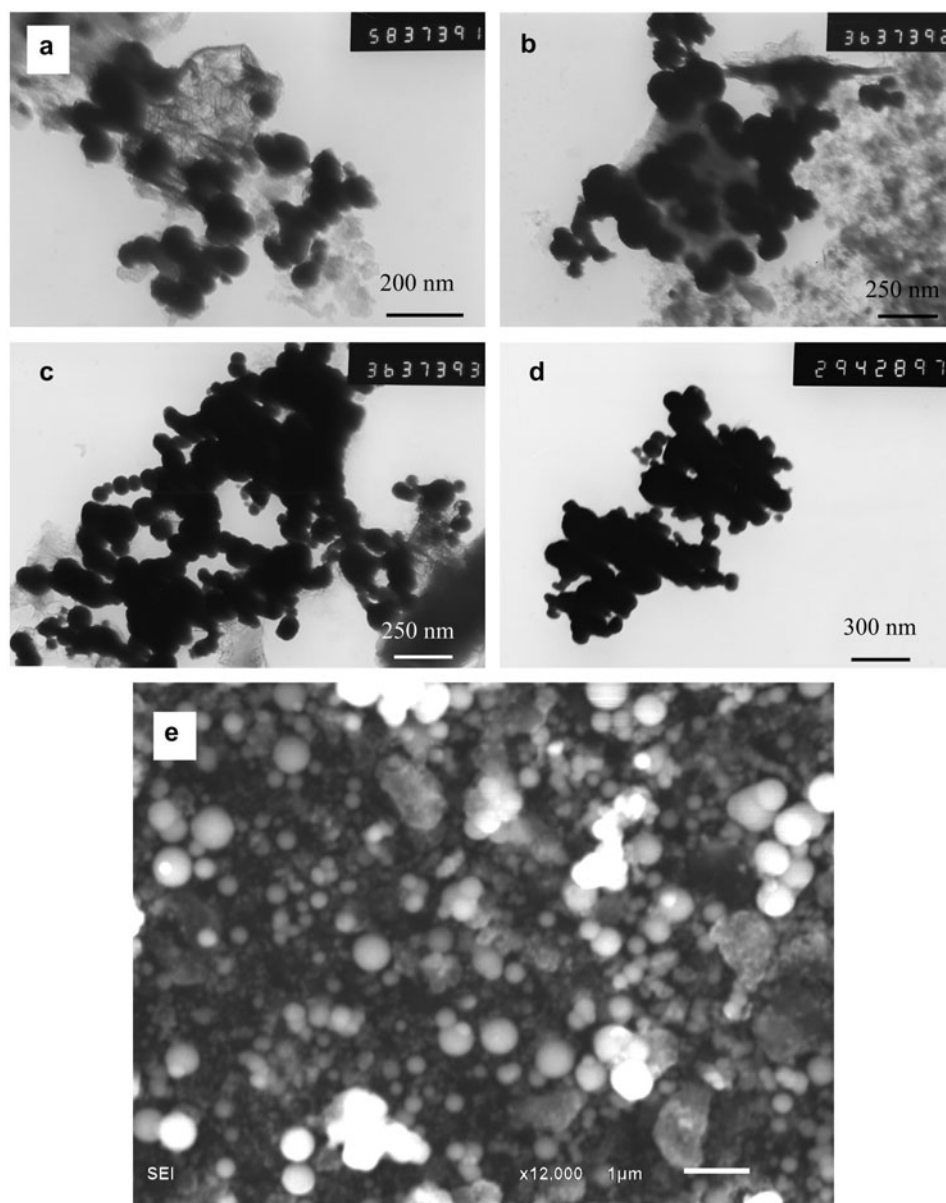


Fig. 2. TEM images of different nZVI/AC samples: (a) nZVI/AC-1; (b) nZVI/AC-2; (c) nZVI/AC-3.

Table 1
The BET surface area of nZVI and different nZVI/AC types

Sample	nZVI	nZVI/AC-1	nZVI/AC-2	nZVI/AC-3
Mass ratio	–	20%	25%	30%
Surface area m^2/g	34.7	50.222	97.468	45.156

with nZVI-1 and nZVI-2. Therefore, nZVI/AC-2 may be a better choice to remove the bromate. The blank experiment was conducted to investigate the corrosion

of nZVI by deionized water at the same condition with nZVI/AC-2. The result reveals that nZVI particles can be oxidized by the oxygen dissolved in

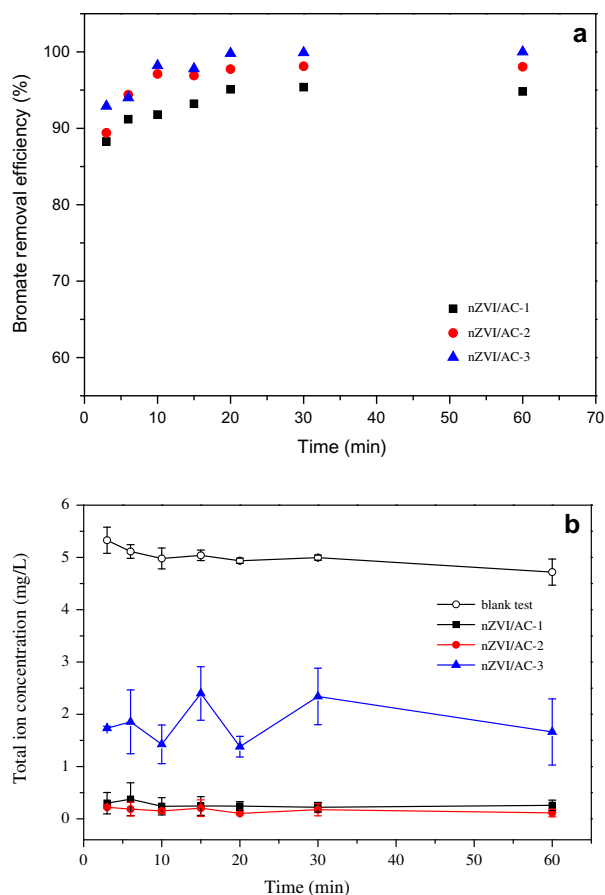


Fig. 3. Effect of nZVI loading on AC on the bromate removal, (a) plots of efficiency of bromate removal vs. contact time; (b) plots of iron concentration vs. contact time. Reaction conditions: initial BrO_3^- concentration 10 mg/L, nZVI/AC dosage 0.4 g/L at 200 rpm, 298 K; blank—deionized water with 0.4 g/L nZVI/AC-2 at 200 rpm, 298 K.

the water, and $\text{Fe}^{2+}/\text{Fe}^{3+}$ were released into the solution. Thus, the total iron concentration in the blank test was high.

Fig. 4 shows the concentration of bromide under different nZVI loading at different reaction time. The results from Figs. 3 and 4 show that there was no mass balance of bromine in the solution, which suggested that the adsorption/co-precipitation of bromate and bromide onto nZVI/AC may appear due to the association of iron oxides [9].

3.2.2. Effect of contact time and dosage

The effect of nZVI/AC-2 dosage on the removal of bromate has been studied at 298 K by varying the nZVI/AC-2 doses from 0.3 to 0.5 g/L (the initial bromate concentration 10 mg/L, pH 7.0 ± 0.1 , 200 rpm). Fig. 5 presents the results. As the amount of nZVI/

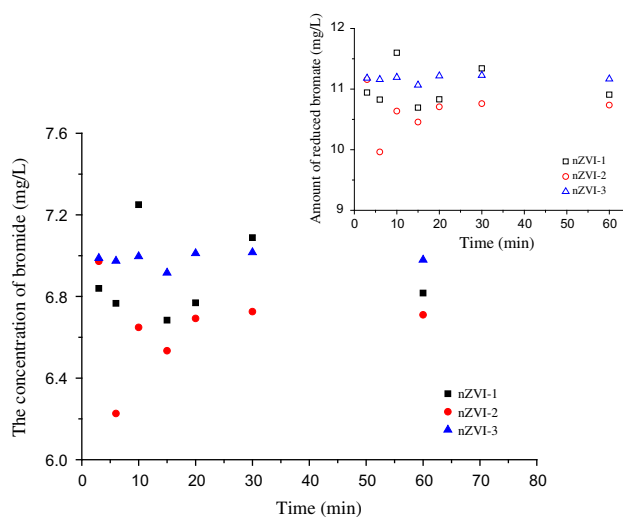


Fig. 4. Plots of the concentration of bromide vs. contact time under different nZVI loading. (Inset: plots of bromate concentration reduced by nZVI/AC materials vs. contact time)

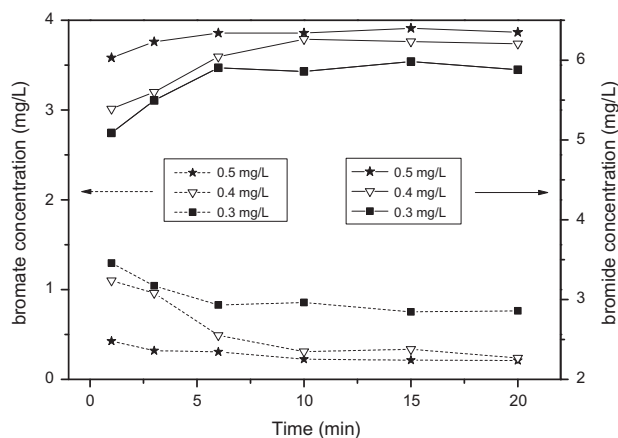


Fig. 5. Effect of nZVI/AC dosage on bromate adsorption/reduction, remaining concentration of BrO_3^- (dashed lines) and concentration of Br^- (solid lines). Reaction conditions: initial BrO_3^- concentration 10 mg/L, nZVI/AC-2 dosage 0.4 g/L, react 20 min at 200 K, 298 rpm.

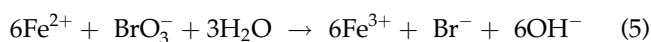
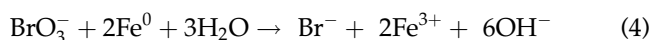
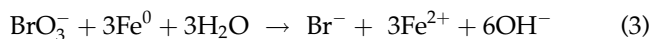
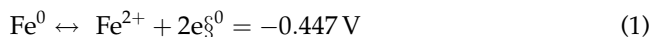
AC-2 increased, the bromate concentration decreased along with the increase in bromide concentration. With the increase of dosage, more nZVI are available for bromate reduction and more AC for adsorption. However, it was noticed that there was no significant increase in the bromate removal at 0.4–0.5 g/L. And the extension of reaction time to 20 min had a little variation to the effluent concentration of bromate and bromide at the same dose. So, an nZVI/AC-2 dose of 0.4 g/L was selected for the further experiments.

3.2.3. Effect of pH

pH is an important controlling parameter in the process of bromate removal. In order to determine the optimum pH range using nZVI/AC-2 as the removal material, the BrO_3^- removal was studied as a function of initial pH. The total iron concentration and the bromide concentration in solution were also detected to find better pH range for BrO_3^- removal.

Fig. 6 shows the adsorption/reduction results of an initial BrO_3^- concentration of 10 mg/L. As observed, at pH of 3.0–9.0, a stable pH zone appeared where the high bromate removal efficiency was obtained. When the initial pH was above 9, a noticeable fall in bromate removal efficiency was found. From pH 3.0–9.0, the remaining bromate concentration was maintained at low concentrations (0.21–0.38 mg/L) and increased sharply to 1.10 mg/L at pH 10.0. In the pH 3.0–5.0, there was a lower bromate concentration compared with pH 6.0–9.0. There maybe two reasons which accelerated the bromate reduction by nZVI at lower pH. First, the iron oxide layers covering the nZVI core dissolves more at lower pH, which in turn renders the nZVI core to rapidly react with bromate. Another reason may be attributed to the ionization of both nZVI/AC and bromate, which caused a repulsion between them when pH of the solution is high [9]. Generally, the net positive charge decreases with increasing pH value and leads to decrease in the repulsion between the adsorbent surface and adsorbate [39]. Wang et al. [40] and Kanel et al. [39] obtained the similar trends using nZVI for bromate and As(III) removal.

The following equations have been suggested as the bromate reduction pathway with ZVI [9]:



Due to the redox potential (Eqs. (1) and (2)), nZVI is easily oxidized to Fe^{2+} . However, an extensive evaluation of bromate reduction using nanoscale zero-valent iron (nZVI) has not been established.

The bromide concentration reduced obviously at pH 10.0. The amount of iron released decreased to 0 mg/L with the pH increasing from 4.0 to 7.0, and then increased slightly when $\text{pH} > 7.0$. Because BrO_3^- reduction accompanies with Br formation, the amount of Br generated in the effluent can be used to calculate the amount of BrO_3^- reduced by nZVI/AC-2. Then, the reduction contribution to the BrO_3^- removal by nZVI/AC-2 was evaluated (Fig. 7). After 20 min, BrO_3^- reacted with nZVI/AC-2 from pH 3 to 9, above 95% bromate removal efficiency was obtained by BrO_3^- reduction, and other BrO_3^- was probably removed by adsorption or co-precipitation. The electrophoretic mobility of pristine nZVI/AC at different initial pH (3.0–9.0) solutions was measured to determine the point of zero charge (PZC). PZC of nZVI/AC was found to be at pH 3.5 (Figure S, Supplemental information).

3.2.4. Effect of bromate initial concentration

Reactions of the different concentrations of bromate with the nZVI/AC-2 were shown in Fig. 8. It showed that bromate was removed rapidly and achieved the equilibrium within 1 min when the initial bromate concentration was 1 and 5 mg/L. When the initial bromate concentration was 10 mg/L, the equilibrium time was 3 min. So, the bromate removal rate was quite high and rapid initially. About 86% of the bromate was removed during the first minute of the reaction when the initial bromate concentration was 1 and 5 mg/L, while a very small part of the additional removal occurred during the following contact. At the initial bromate concentration 10 mg/L, 82% was removed during the first minute.

Fig. 8 also showed the reduction/adsorption was strongly dependent on the initial bromate concentration. For initial bromate concentration of 1, 5, and 10

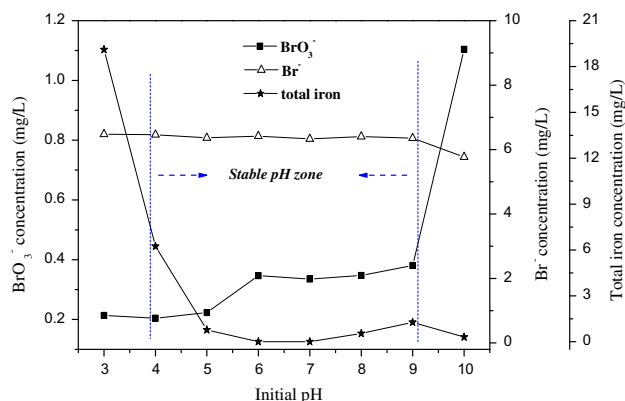


Fig. 6. BrO_3^- adsorption/reduction by nZVI/AC-2, and the formation volume of Br^- . Reaction conditions were same as in Fig. 5.

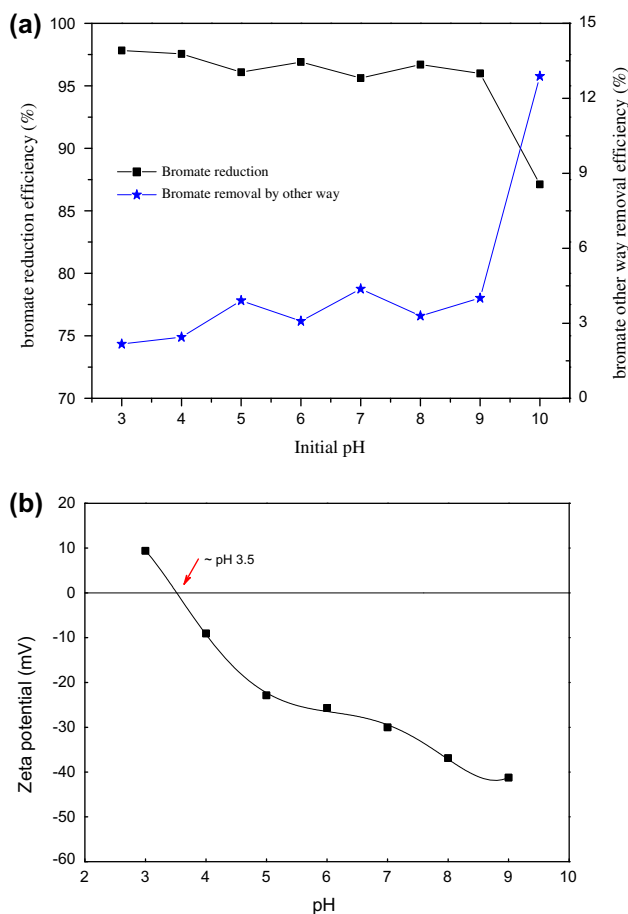


Fig. 7. (a) Effect of pH on bromate removal. (Reaction conditions were same as that of Fig. 5. (b) Electrophoretic mobility of nZVI/AC with respect to pH.

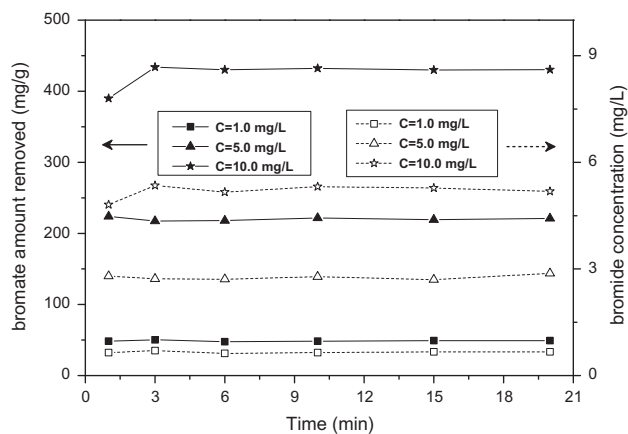


Fig. 8. Effect of reaction time and initial concentration for bromate adsorption/reduction using nZVI/AC-2. Reaction conditions: nZVI/AC-2 dosage 0.4 g/L, react at 200 rpm, 298 K.

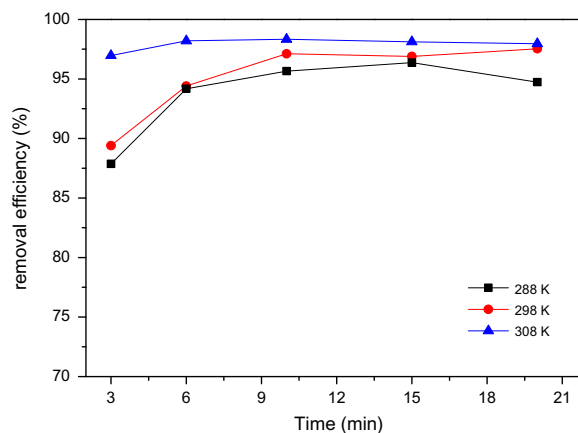


Fig. 9. Effect of contact time and reaction temperature for bromate removal using nZVI/AC-2 as removal material. Reaction conditions: initial bromate concentration 10 mg/L, nZVI/AC-2 dosage 0.4 g/L, reacted at 200 rpm.

mg/L, the bromate amount removed at 3 min were 50.37 mg/g, 217.42 mg/g, and 433.90 mg/g, respectively. The driving force of the concentration gradient increased with the increase of the BrO_3^- initial concentration to overcome the mass transfer resistance in the liquid-solid phase system [39]. Therefore, higher initial bromate concentration may increase the removal capacity. Compared with the equilibrium time for bromate removal using nZVI [8,10], the equilibrium time using composite material is much shorter.

3.2.5. Effect of temperature

The effects of temperature were studied for bromate removal using nZVI/AC as removal material at different temperature and different contact time (Fig. 9). Fig. 9 shows the bromate removal efficiency was 98.3, 97.1, and 95.6%, respectively under 308, 298, and 288 K within 10 min, so the equilibrium was achieved within a short time. But at 288 K, 15 min was required to achieve the maximum removal efficiency (94.4%). Since high temperature favors the bromate removal, the adsorption process is endothermic. The bromate removal occurred quickly and the time required to achieve equilibrium is relevant with reaction temperature.

4. Conclusions

In general, AC can be a carrier for nZVI to synthesize a novel nanocomposite material, which effectively prevented the agglomeration of nano metal such as the non-supported nZVI. Batch experiments

were performed under different physico-chemical conditions (adsorbent dosage, pH, initial bromate concentration, temperature and contact time) using prepared adsorbents. Results indicated that nZVI/AC can effectively remove bromate from water, possessing higher removal efficiency than AC. BrO_3^- was reduced immediately by Fe^0 to Br^- and adsorbed on the surface of AC and Fe^0 simultaneously. Bromate removal is favored under acidic pH values, but the studied materials are effective over wide range of pH. Bromate removal is favored when the initial concentration of bromate or temperature of solution increased. nZVI/AC could be a promising material for water purification containing persistent toxic pollutants due to its significant reduction reactivity and adsorption capacity.

Acknowledgments

This research was supported by the National Natural Science Foundation of China (Grant No. 51102157), Shandong Key Scientific and Technological Development Plan of China (2013GSF11708). This study was also funded by National Major Special Technological Programs Concerning Water Pollution Control and Management in the Twelfth Five-year Plan Period (No. 2012 ZX07203-004).

References

- [1] US EPA, Guidelines for carcinogen risk assessment, Federal Register 51, US Environmental Protection Agency, 1986, pp. 33992–34003
- [2] R. Butler, S. Ehrenberg, A.R. Godley, R. Lake, L. Lytton, E. Cartmell, Remediation of bromate-contaminated groundwater in an ex situ fixed-film bioreactor, *Sci. Total. Environ.* 366 (2006) 12–20.
- [3] H.S. Weinberg, C.A. Delcomyn, V. Unnam, Bromate in chlorinated drinking waters: Occurrence and implications for future regulation, *Environ. Sci. Technol.* 37 (2003) 3104–3110.
- [4] D. Delker, G. Hatch, J. Allen, B. Crissman, M. George, D. Geter, S. Kilburn, T. Moore, G. Nelson, B. Roop, R. Slade, A. Swank, W. Ward, A. DeAngelo, Molecular biomarkers of oxidative stress associated with bromate carcinogenicity, *Toxicology* 221 (2006) 158–165.
- [5] W.H. Glaze, H.S. Weinberg, J.E. Cavanagh, Evaluating the formation of brominated DBPs during ozonation, *J. Am. Water Works Assoc.* 85 (1993) 96–103.
- [6] W.J. Huang, Y.L. Cheng, Effect of characteristics of activated carbon on removal of bromate, *Sep. Purif. Technol.* 59 (2008) 101–107.
- [7] A. Bhatnagar, Y.H. Choi, Y.J. Yoon, Y. Shin, B.H. Jeon, J.W. Kang, Bromate removal from water by granular ferric hydroxide (GFH), *J. Hazard. Mater.* 170 (2009) 134–140.
- [8] Q.L. Wang, S. Snyder, J.W. Kim, H. Choi, Aqueous ethanol modified nanoscale zerovalent iron in bromate reduction: Synthesis, characterization, and reactivity, *Environ. Sci. Technol.* 43 (2009) 3292–3299.
- [9] L. Xie, C. Shang, Effects of copper and palladium on the reduction of bromate by Fe^0 , *Chemosphere* 64 (2006) 919–930.
- [10] L. Xie, C. Shang, The effects of operational parameters and common anions on the reactivity of zero-valent iron in bromate reduction, *Chemosphere* 66 (2007) 1652–1659.
- [11] P.C. Singer, K. Bilyk, Enhanced coagulation using a magnetic ion exchange resin, *Water Res.* 36 (2002) 4009–4022.
- [12] C.J. Johnson, P.C. Singer, Impact of a magnetic ion exchange resin on ozone demand and bromate formation during drinking water treatment, *Water Res.* 38 (2004) 3738–3750.
- [13] S. Peldszus, S.A. Andrews, R. Souza, F. Smith, I. Douglas, J. Bolton, P.M. Huck, Effect of medium-pressure UV irradiation on bromate concentrations in drinking water, a pilot-scale study, *Water Res.* 38 (2004) 211–217.
- [14] H. Noguchi, A. Nakajima, T. Watanabe, K. Hashimoto, Design of a photocatalyst for bromate decomposition: Surface modification of TiO_2 by pseudo-boehmite, *Environ. Sci. Technol.* 37 (2003) 153–157.
- [15] C. Noubactep, An analysis of the evolution of reactive species in $\text{Fe}^0/\text{H}_2\text{O}$ systems, *J. Hazard. Mater.* 168 (2009) 1626–1631.
- [16] Y.H. Kim, E.R. Carraway, Dechlorination of pentachlorophenol by zero valent iron and modified zero valent irons, *Environ. Sci. Technol.* 34 (2000) 2014–2017.
- [17] W.Z. Yin, J.H. Wu, P. Li, X.D. Wang, N.W. Zhu, P.X. Wu, B. Yang, Experimental study of zero-valent iron induced nitrobenzene reduction in groundwater: The effects of pH, iron dosage, oxygen and common dissolved anions, *Chem. Eng. J.* 184 (2012) 198–204.
- [18] Y. Wang, D.M. Zhou, Y.J. Wang, X.D. Zhu, S.Y. Jin, Humic acid and metal ions accelerating the dechlorination of 4-chlorobiphenyl by nanoscale zero-valent iron, *J. Environ. Sci.* 23 (2011) 1286–1292.
- [19] H. Song, E.R. Carraway, Reduction of chlorinated ethanes by nanosized zero-valent iron: Kinetics, pathways, and effects of reaction conditions, *Environ. Sci. Technol.* 39 (2005) 6237–6245.
- [20] J. Farrell, N. Melitas, M. Kason, T. Li, Electrochemical and column investigation of iron-mediated reductive dechlorination of trichloroethylene and perchloroethylene, *Environ. Sci. Technol.* 34 (2000) 2549–2556.
- [21] S.Y. Oh, S.G. Kang, P.C. Chiu, Degradation of 2,4-dinitrotoluene by persulfate activated with zero-valent iron, *Sci. Total. Environ.* 408 (2010) 3464–3468.
- [22] J. Farrell, J.P. Wang, P. O'Day, M. Conklin, Electrochemical and spectroscopic study of arsenate removal from water using zero-valent iron media, *Environ. Sci. Technol.* 35 (2001) 2026–2032.
- [23] C.M. Su, R.W. Puls, Arsenate and arsenite removal by zerovalent iron: Effects of phosphate, silicate, carbonate, borate, sulfate, chromate, molybdate, and nitrate, relative to chloride, *Environ. Sci. Technol.* 35 (2001) 4562–4568.
- [24] M.S.H. Mak, I.M.C. Lo, Influences of redox transformation, metal complexation and aggregation of fulvic acid and humic acid on Cr(VI) and As(V) removal by zero-valent iron, *Chemosphere* 84 (2011) 234–240.

- [25] T. Suzuki, M. Moribe, Y. Oyama, M. Niinae, Mechanism of nitrate reduction by zero-valent iron: Equilibrium and kinetics studies, *Chem. Eng. J.* 183 (2012) 271–277.
- [26] Y. An, T.L. Li, Z.H. Jin, M.Y. Dong, Q.Q. Li, S.M. Wang, Decreasing ammonium generation using hydrogenotrophic bacteria in the process of nitrate reduction by nanoscale zero-valent iron, *Sci. Total Environ.* 407 (2009) 5465–5470.
- [27] K.L. McGeough, R.M. Kalin, P. Myles, Carbon disulfide removal by zero valent iron, *Environ. Sci. Technol.* 41 (2007) 4607–4612.
- [28] Y.Q. Zhang, C. Amrhein, W.T. Frankenberger Jr, Effect of arsenate and molybdate on removal of selenate from an aqueous solution by zero-valent iron, *Sci. Total Environ.* 350 (2005) 1–11.
- [29] H.J. Zhu, Y.F. Jia, X. Wu, H. Wang, Removal of arsenic from water by supported nano zero-valent iron on activated carbon, *J. Hazard. Mater.* 172 (2009) 1591–1596.
- [30] L.B. Hoch, E.J. Mack, B.W. Hydutsky, J.M. Hershman, J.M. Skluzacek, T.E. Mallouk, Carbothermal synthesis of carbon-supported nanoscale zero-valent iron particles for the remediation of hexavalent chromium, *Environ. Sci. Technol.* 42 (2008) 2600–2605.
- [31] L.N. Shi, Y.M. Lin, X. Zhang, Z.L. Chen, Synthesis, characterization and kinetics of bentonite supported nZVI for the removal of Cr(VI) from aqueous solution, *Chem. Eng. J.* 171 (2011) 612–617.
- [32] S.M. Ponder, J.G. Darab, T.E. Mallouk, Remediation of Cr(VI) and Pb(II) aqueous solutions using supported, nanoscale zero-valent iron, *Environ. Sci. Technol.* 34 (2000) 2564–2569.
- [33] Z.M. Gu, J. Fang, B.L. Deng, Preparation and evaluation of GAC-based iron-containing adsorbents for arsenic removal, *Environ. Sci. Technol.* 39 (2005) 3833–3843.
- [34] W. Wang, Z.H. Jin, T.L. Li, H. Zhang, S. Gao, Preparation of spherical iron nanoclusters in ethanol–water solution for nitrate removal, *Chemosphere* 65 (2006) 1396–1404.
- [35] L.N. Shi, X. Zhang, Z.L. Chen, Removal of Chromium (VI) from wastewater using bentonite-supported nanoscale zero-valent iron, *Water Res.* 45 (2011) 886–892.
- [36] K. Mackenzie, S. Bleyl, A. Georgi, F.D. Kopinke, Carbo-iron—An Fe/AC composite—As alternative to nano-iron for groundwater treatment, *Water Res.* 46 (2012) 3817–3826.
- [37] B. Geng, Z.H. Jin, T.L. Li, X.H. Qi, Kinetics of hexavalent chromium removal from water by chitosan-Fe⁰ nanoparticles, *Chemosphere* 75 (2009) 825–830.
- [38] K.D. Hristovski, P.K. Westerhoff, T. Möller, P. Sylvester, Effect of synthesis conditions on nano-iron (hydr)oxide impregnated granulated activated carbon, *Chem. Eng. J.* 146 (2009) 237–243.
- [39] E. Demirbas, N. Dizge, M.T. Sulak, M. Kobya, Adsorption kinetics and equilibrium of copper from aqueous solutions using hazelnut shell activated carbon, *Chem. Eng. J.* 148 (2009) 480–487.
- [40] W. Wang, Z.H. Jin, T.L. Li, H. Zhang, S. Gao, Preparation of spherical iron nanoclusters in ethanol–water solution for nitrate removal, *Chemosphere* 65 (2006) 1396–1404.